Desalination and Water Treatment
www.deswater.com

doi:10.5004/dwt.2018.22753

120 (2018) 311–322
July

Influence of infiltration rates during profenofos pesticide removal by attached and entrapped bacterial cells

K. Sonsuphab[a], T. Ratpukdi[a,b], S. Siripattanakul–Ratpukdi[a,b,*]

[a]*Department of Environmental Engineering, Faculty of Engineering and Research Center for Environmental and Hazardous Substance Management, Khon Kaen University, Khon Kaen 40002, Thailand, Tel. +664 320 2572,*
email: pangzazz_kp@hotmail.com (K. Sonsuphab), thunyalux@kku.ac.th (T. Ratpukdi)
[b]*Center of Excellence on Hazardous Substance Management, Bangkok 10330, Thailand, Tel. +664 320 2572, Fax +664 320 2571,*
email: sumana.r@kku.ac.th, jeans_sumana@yahoo.com (S. Siripattanakul-Ratpukdi)

Received 29 December 2017; Accepted 1 July 2018

ABSTRACT

Profenofos (O-4-bromo-2-chlorophenyl-O-ethyl S-propyl phosphorothioate) is a widely used organophosphorus pesticide for agricultural purpose. This caused contamination in subsurface system. This study investigated profenofos pesticide remediation by attached and entrapped bacterial cells compared to the treatment by free cells. Influence of infiltration rates (1–5 cm d^{-1}) on profenofos removal was focused. *Pseudomonas aeruginosa* strain PF2, a profenofos–degrading culture, was chosen. Peanut shell as a support material for the attached cells and barium alginate as a matrix for the entrapped cells were applied in sand column experiment. During the column experiment at the infiltration rate of 1 cm d^{-1}, profenofos removal by all tests was high (94–97%). For infiltration rates of 3 and 5 cm d^{-1}, the free cells could remove profenofos of 50–71% while the immobilized cell systems (the attached and entrapped cells) obviously improved the profenofos removal (90–97%). This is because high cell retention in the immobilized cell systems and profenofos adsorption by the immobilization materials. The long-term experiment further proved that the cell entrapment using barium alginate better increased cell retention and reduced the impact of profenofos toxicity leading to better profenofos removal performance.

Keywords: Alginate; Biofilm; Bioremediation; Organophosphorus; Peanut shell

1. Introduction

Organophosphorus pesticides have long been used for agricultural purpose [1]. Among them, profenofos (O-4-bromo-2-chlorophenyl-O-ethyl S-propyl phosphorothioate) is largely applied in many countries [1,2]. This resulted in profenofos contamination over allowable concentration (3 μg L^{-1}) in environment including surface water and groundwater [1–3]. Groundwater is a major drinking water source in remote area. Consumption of profenofos-contaminated groundwater could cause adverse health effect since profenofos was classified by The World Health Organization as a neurotoxic substance. Therefore, the profenofos-contaminated site remediation is needed.

One of effective *in situ* treatment technologies is microbial remediation. This technique uses microorganisms to transform pollutants to be less or non-toxic substances. The microorganisms can be inoculated in the soil at top zone to degrade contaminant in soil and infiltrate before reaching to groundwater level (Fig. 1). In reality, the free microbial cells could move out of the contaminated sites resulting in decreasing contaminant removal performance [4]. To maintain the efficiency of microbial remediation, the cell retention at the remediation site is necessary. Cell immobilization, a cell retention method, is broadly used for

*Corresponding author.

environmental applications including water purification, wastewater treatment, and site remediation. Among the immobilization techniques, cell attachment and cell entrapment were the most commonly practical techniques [5]. The cell attachment is to grow the microorganisms (biofilm) on support materials while the cell entrapment is to mix the microorganisms and form the polymeric gel beads (with cells). Advantages of these techniques are high microbial cell retention and no reaction (damage) to microbial cells during the cell immobilization processes [6]. Also, these techniques have been successfully applied for treating numerous pollutants, such as crude oil hydrocarbon, atrazine, and profenofos [6–8].

These cell immobilization techniques (cell attachment and cell entrapment) have potential for remediating profenofos-contaminated in top zone. In practice, there was no clear criteria about suitable immobilization technique. Some different limitations of both techniques were reported. In case of the entrapped cells, the restriction of substrate diffusion into the entrapment matrix could limit the cell growth and degradation efficiency whereas biofilm may be easily washed off the cell attachment system [9]. Thus far, no comparative study of the cell entrapment and cell attachment for the site remediation has been investigated. To achieve the subsurface remediation, infiltration rate was an important factor since it related to hydraulic conductivity which has impact on fate, transport, and treatment of contaminants in soil and groundwater [4,10].

This study aims to investigate profenofos removal performance by the attached and entrapped cells. The sand column experiment by the immobilized (attached and entrapped) cells was performed in comparison of the free cell experiment. This work focused on the remediation under influence of infiltration rates. *Pseudomonas aeruginosa* strain PF2 (PF2), a previously isolated profenofos-degrading bacterium, was chosen [2]. Based on the literatures, peanut shell and barium alginate were selected as a support material for the attached cells and a matrix for cell entrapment, respectively [8,11]. The result from this study will be useful for site remediation practice in the future.

2. Materials and methods

2.1. Bacterial strain and cultural condition

A previously isolated profenofos-degrading bacterium, PF2 (GenBank accession number KJ143903), was chosen based on high profenofos-degrading performance [2]. A minimal salt medium for bacterium cultivation was prepared in a phosphate buffer solution (10 mM, pH of 6.8). The medium comprising $MgSO_4 \cdot 7H_2O$ 0.513 g L^{-1}, NaCl 0.5 g L^{-1}, KH_2PO_4 3.0 g L^{-1}, $NaH_2PO_4 \cdot 2H_2O$ 6.815 g L^{-1}, NH_4Cl 2 g L^{-1}, and filtered sterile profenofos of 20 mg L^{-1} was used. The bacterium at the late exponential phase was cultivated using orbital shaker at 150 rpm under room temperature for 3 d before experiment followed method described elsewhere [2].

For the experiment, the cultivated PF2 was centrifuged at a 6,000 rpm for 10 min to obtain concentrated cell suspension. The concentrated cells were applied as initial free PF2 cells (10^{12} CFU m L^{-1}). Also, the concentrated cells were used for preparing attached and entrapped cells.

2.2. Cell immobilization procedures

2.2.1. Cell attachment

Peanut shells (obtained from a local market in Khon Kaen, Thailand) were washed with tap water and dried in oven at 60°C for 6 h. Then, the dried peanut shell was cut into small pieces and sieved using USA standard sieves number 4 and 8 to obtain the peanut shell sizes of 2–5 mm. The materials were then sterilized by autoclaved at 121°C for 20 min twice for two consecutive days. To form biofilm, the concentrated PF2 cells (10^{12} CFU m L^{-1} in 100-m L medium) were mixed with the autoclaved peanut shell of 10 g and incubated for 5 d by shaking at 150 rpm and room temperature. The peanut shell-attached cells at 5-d shaking were 10^{11} CFU mL-medium^{-1}. Potential of biofilm formation and cell growth were daily checked using alcian blue adsorption assay (supplementary material) and spread plate count, respectively.

2.2.2. Cell entrapment

To prepare barium alginate-entrapped cell, a sodium alginate solution of 3% (w/v) (Sigma-Aldrich, Singapore) was mixed with the concentrated PF2 of 10^{12} CFU mL^{-1}. The ratio of sodium alginate and the concentrated PF2 cells was 10:1 (by volume). The mixture was dropped into a barium chloride ($BaCl_2$) solution of 5% (w/v) (Sigma-Aldrich, Singapore) using a 10-mL sterile syringe to form spherical beads with a size of about 3 mm. The beads were hardened in the $BaCl_2$ solution for 2 h [11].

2.3. Experimental preparation and setup

2.3.1. Sand preparation

To avoid influence of soil properties on profenofos biodegradation, silica sand (industrial grade) of 300 mL was used as a subsurface medium. Sand preparation procedure was followed Siripattanakul et al. [4]. The sand was washed, oven-dried at 105°C for 24 h, and baked at 550°C for 1 h (3 times). The baked sand was sieved by USA standard sieves number 35 and 60 to obtain particle sizes of 0.25–0.45 mm (porosity of 33.33%) and then autoclaved at 121°C for 20 min for 3 times.

2.3.2. Column preparation, setup, and operation

A polypropylene column (diameter of 5 cm and length of 22 cm) was used to simulate subsurface system (Fig. 1). The column was soaked with 70% ethanol and rinsed with sterilized de-ionized water before use. The autoclaved sand of 300 mL was mixed with free, attached, or entrapped cells before packing into the column. Composition in each column is presented in Table 1. The cell and sand mixture was loosely packed into the column for 20-cm length. It is noted that a sand column without cell and material was added in the control test. The packed column was wrapped using aluminum foil to prevent profenofos photolysis.

The column operation was followed Siripattanakul et al. [4]. The minimal salt medium as synthetic contaminated water was down–flowed through the column under step-

feed mode. The contaminated water of 8, 20, and 35 mL was poured into column at 8-h interval to simulate the contaminated infiltrate at infiltration rates of 1, 3, and 5 cm d^{-1}, respectively. It is noted that the range of infiltration rates was selected based on typical average precipitation. The selected water infiltration rates of 1, 3, and 5 cm d^{-1} were equivalent to water seepage of approximately 0.2, 0.6, and 1.0 pore (water) volume (PV) per day, respectively.

2.4. Chloride and profenofos tracer tests under different infiltration rates

Before the profenofos biodegradation experiment, examination of contaminant transport in the column was required. Triplicate chloride and profenofos tracer tests in the sand column were performed to represent hydraulic and contaminant transports, respectively. It is noted that pH of the medium applied in this study was controlled at about neutral to avoid natural hydrolysis of profenofos.

A calcium chloride solution of 0.01 M was fully filled into the sand column. Then, the calcium chloride solution of 0.05 M and the profenofos solution of 20 mg L^{-1} were down flow-fed at the infiltration rates of 1, 3, and 5 cm d^{-1} through the sand column. A step-feed mode followed Siripattanakul et al. was applied [4]. The effluent samples were continuously taken for measuring electrical conductivity and profenofos concentration from chloride and profenofos tracer tests, respectively. Profenofos (or chloride) concentration was calculated as normalized remained concentration followed Eq. (1). C is profenofos (or chloride) concentration (mg L^{-1}) at a time whereas C_0 is the initial profenofos (or chloride) concentration (mg L^{-1}).

$$Normalized\ remained\ profenofos\ concentration = \frac{C}{C_0} \quad (1)$$

The breakthrough curves of the tracer test were completed. Normalized remained concentration (C/C_0) were plotted against PV. To interpret the contaminant transport, retardation factor (R_f) of profenofos was calculated following Eq. (2). The profenofos removal efficiency was calculated as shown in Eq. (3).

$$R_f = \frac{PV_{Profenofos\ at\ \frac{C}{C_0}=0.5}}{PV_{Chloride\ at\ \frac{C}{C_0}=0.5}} \quad (2)$$

$$Profenofos\ removal\ efficiancy = \frac{C_0 - C}{C_0} \times 100 \quad (3)$$

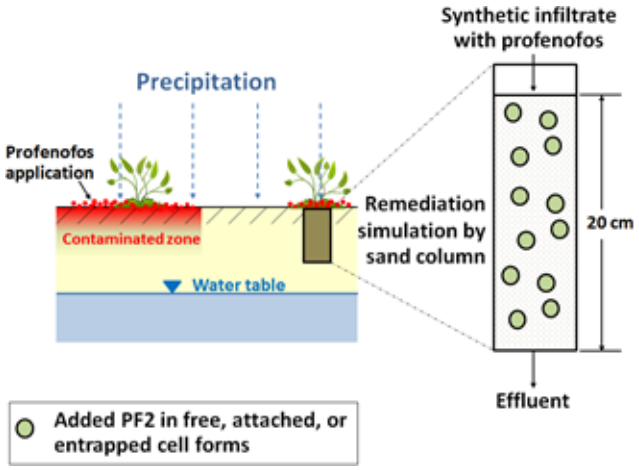

Fig. 1. Schematic diagram of sand column for subsurface system simulation.

2.5. Profenofos removal experiment under different infiltration rates

Triplicate profenofos removal experiments were carried out. Five different setups including 1) the free cells (**FC**) (concentrated PF2 as mentioned earlier), 2) peanut shell–attached cells (**AC**), 3) barium alginate-entrapped cells (**EC**), 4) peanut shells (no cell) (**PS**), and 5) barium alginate (no cell) (**BA**) were prepared. The influence of infiltration rates on the profenofos removal performance and cell leaching were studied. Initial cell number of 10^{11} CFU m L^{-1} in the column was controlled for the free, attached, and entrapped cell tests.

At the beginning, the columns were filled up by the synthetic infiltrate without profenofos. For the short-term tests, the profenofos-contaminated infiltrate with infiltration rates of 1, 3, and 5 cm d^{-1} was downward step-fed through the column for 5 PV. The column effluent was continuously sampled to measure the leaching cell number and profenofos concentration.

The long term (50 PV) monitoring tests were selected only an infiltration rate based on the short-term result (the most influenced rate on profenofos removal efficiency). The

Table 1
Composition of tracer, FC, AC, EC, PS, and BA columns

Test	Description	Material and sand mixture (mL)	Immobilization material (g as dried weight)	Material volume (mL)	Cell number (CFU mL^{-1})
Tracer	Only sand for tracer (or control) tests	300	0	0	0
FC	Free cell tests	300	0	0	10^{12}
AC	Peanut shell-attached cell tests	300	10	10	10^{12}
PS	Only peanut shell tests (no added cell)	300	10	10	0
EC	Barium alginate-entrapped cell tests	300	10	100	10^{12}
BA	Only barium alginate tests (no added cell)	300	10	100	0

column was operated in the same manner to the short-term test. The leaching cell number and profenofos concentration were detected daily. Micro-structural observation of the immobilized cells was performed using scanning electron microscope (SEM).

2.6. Analytical methods

The free PF2 cells were counted using typical spread plate count technique. The solid medium (section 2.1) was added 2% of agar. For the attached PF2 on peanut shells, the PF2 cells were extracted. The attached cell samples of 5 pieces in bacterial medium of 1 mLwere added into a 1.5-mL centrifuge tube and soaked for 3 min. Then, the samples were sonicated using ultrasonic bath (Fisher Scientific, 136H, USA) for 2 min and shaken on a vortex mixer for 2 min. The cell extraction process was repeated twice for each step. After that, the de-immobilized PF2 cells were serially diluted and spread-plated.

For profenofos measurement, the samples were extracted using liquid–liquid extraction technique. Hexane was applied as an extraction solvent followed previous studies [1,2]. The sample of 0.5 mL was mixed with hexane (containing acetic acid of 0.01% (by volume)) of 0.5 mL. After mixing and settling the sample-solvent sample, upper phase of mixture (hexane) was drawn for 200 µL and filtered. A gas chromatography (GC) (4890D, Agilent Technologies, USA) with electron capture detector and SPB-608 fused silica capillary column (15-m length, 0.53-mm I.D., and d_f of 0.50) was used. Helium and nitrogen gases were used as the carrier gases with flow rates of 8 mL min^{-1} and 47 mL min^{-1}, respectively. One micro liter of sample was injected to the GC. The injection port and detector temperatures of 240°C and 250°C, respectively were set. The GC program was started at 120°C, hold at 120°C for 2 min, raised to 240°C at a rate of 40°C min^{-1}, and hold for 5 min. Profenofos peak was at 3.1 min. The average method recovery for profenofos concentrations of 1–20 mg L^{-1} was 80%.

For immobilized cell observation using SEM, the attached and entrapped cell samples of 5 pieces were washed in a solution containing NaCl of 0.85% (w/v) and $BaCl_2$ of 5% (w/v) and then washed with sterilized de-ionized water. The washing process was repeated three times. Then, the sample were dried in hot air oven (UF160, Memmert, Germany) at 60°C for 12 h. The dried beads were cut using a razor blade, attached to a stub, and coated with gold. The dried beads were observed for microbial cell and bead physiology using SEM (S-3000N, Hitachi, Japan).

2.7. Statistical analysis

Data from the experiments were statistically analyzed using STATA10 (StataCorp, College Station, USA). The results were analyzed using a multiple regression model. The difference of profenofos concentrations was examined by one way-ANOVA.

3. Results and discussion

3.1. Profenofos and chloride tracer tests

The effect of infiltration rates (1, 3, and 5 cm d^{-1}) on hydraulic and contaminant transport was investigated using chloride (conservative solute) and profenofos tracer tests, respectively. Fig. 2 is column breakthrough result. Ratios of the concentration at a time respected to the initial concentration (C/C_0) are presented in Fig. 2. It was found that chloride early appeared at 0.25 PV and reached plateau at 2.00 PV for all tests. For profenofos, the leaching concentration increased with rising PV at infiltration rates of 1 and 3 cm d^{-1} whereas profenofos reached plateau at 4.00 PV at infiltration rate of 5 cm d^{-1}. Ideally, for one-dimensional transport model (advection–dispersion), Water (pore) volume through column (x axis) at $C/C_0 = 0.50$ is approximately 1.00 PV. In this study, C/C_0 of 0.50 at the infiltration rates of 1, 3, and 5 cm d^{-1} shifted to 0.70, 1.10, and 1.20 PV, respectively. For profenofos tracer tests, it is obvious that the contaminant transport was slower than the conservative solute transport (Fig. 2). The R_f values at the infiltration rates of 1, 3 and 5 cm d^{-1} were 5.80, 2.40, and 2.50, respectively. Profenofos retardation might be influence of contaminant itself or sand properties. The influence of contaminant retardation should be further examined.

Based on the results in Fig. 2, the mechanical dispersion and diffusion played a role on the delay of hydraulic transport. Infiltration rates directly related to mechanical dispersion. Higher infiltration (flow) rates resulted in higher mechanical dispersion. Deviances from the ideal case could result from diffusion process because of the step–feed operation as well. For the profenofos transport, it is slower than the chloride transport. This phenomenon was typically found in longitudinal transport [13]. Lower infiltration

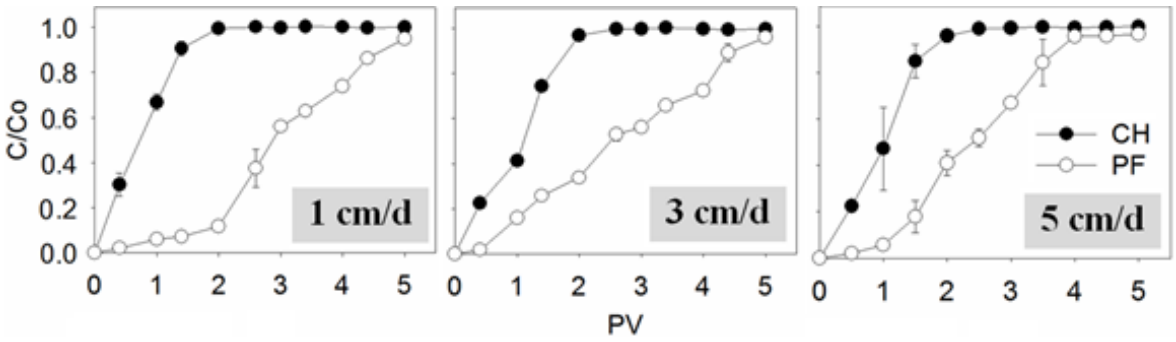

Fig. 2. Breakthrough curves of chloride (CH) and profenofos (PF) tracer tests at the infiltration rates of 1, 3, and 5 cm d^{-1}.

rate (higher water residence times) significantly increased adsorption capacity.

3.2. Profenofos removal under different infiltration rates

Sand column experiments for profenofos removal by the free cells, peanut shell-attached cells, barium alginate-entrapped cells, peanut shells (no cell), and barium alginate (no cell) (called FC, AC, EC, PS, and BA, respectively) were performed. The initial cell number of 10^{11} CFU m L^{-1} and the initial profenofos concentration of 20 mg L^{-1} were applied for the tests. It is noted that the attached cells was to cultivate the PF2 cells on peanut shells before use. Therefore, to control equivalent initial cell number for all tests (the free, attached, and entrapped cells), additional experiment on PF2 growth and biofilm formation on the peanut shells was carried out (supplementary information). Fig. S1 is the results of on PF2 growth and biofilm formation during the preparation of the attached cells used in this study. The PF2 cell number and alcian blue reduction results were well correlated. PF2 increased from approximately 8–11 log CFU g-peanut $shell^{-1}$ at the fifth day while biofilm formation (alcian blue reduction) also increased and reached steady state at the same time. Also, adsorption capabilities of PS and BA were preliminarily determined for better interpretation of profenofos removal mechanism. Fig. S2 clearly proved high profenofos adsorption by PS and BA. Both material had similar adsorption capability of 1.7–1.8 mg-profenofos g-$material^{-1}$ (Table S1).

The profenofos removal by FC, AC, EC, PS, and BA is presented in Fig. 3. All tests were reached plateau within 4 PV. In overall, all sand column tests well removed profenofos for entire of the experiment (5 PV) compared to the tracer result presented in Fig. 2. The profenofos removal efficiencies of 50–97% were observed. The profenofos removal at a stable period (5 PV) is shown in Table 2. During the tests at infiltration rate of 1 cm d^{-1}, profenofos removal in all tests was relatively high (Table 2). The profenofos removal performances by the free cells and immobilized cells (AC and EC) were not significantly different (p = 0.012). This could be from the biodegradation by PF2 and adsorption by the immobilization materials (peanut shells and barium alginate) [4,12]. For the sand column tests at infiltration rates of 3 and 5 cm d^{-1}, the immobilized cell columns (AC and EC)

Table 2
Profenofos removal efficiencies by FC, AC, EC, PS, and BA tests at 5 PV at different infiltration rates

Test	Description	Infiltration rate (cm d^{-1})	Profenofos removal efficiencies (%)
FC	Free cell tests	1	94
		3	71
		5	50
AC	Peanut shell-attached cell tests	1	96
		3	94
		5	90
PS	Peanut shell (no added cell) tests	1	93
		3	89
		5	85
EC	Barium alginate-entrapped cell tests	1	95
		3	97
		5	96
BA	Barium alginate (no added cell) tests	1	84
		3	90
		5	89
Tracer	Profenofos tracer tests (sand only)	1	5
		3	4
		5	3

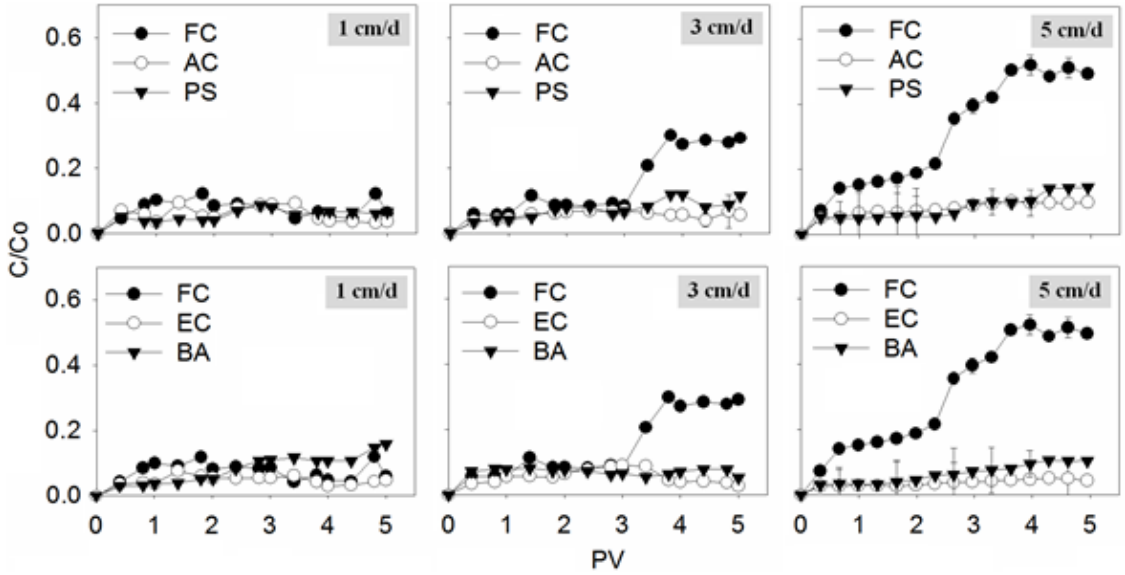

Fig. 3. Breakthrough curves during profenofos removal by the free cell (FC), peanut shell-attached cell (AC), barium alginate-entrapped cell (EC), peanut shell (PS), and barium alginate (BA) tests at the infiltration rates of 1, 3, and 5 cm d^{-1}.

apparently maintained the profenofos removal efficiencies. The results by AC and EC were persistently high for entire of the 5-PV experiment (90–97%). Both immobilization techniques provided insignificantly different performance (p = 0.100) whereas the removal efficiencies by FC were much different (only 50 and 71% for infiltration rates of 3 and 5 cm d^{-1}, respectively).

Fig. 4 shows leaching cell numbers from the FC, AC, and EC columns during profenofos removal under infiltration rates of 1, 3, and 5 cm d^{-1}. The leaching cell numbers from the FC system (9–12 CFU m L^{-1}) decreased at the beginning period and remained stable thereafter. The numbers of cell leaching at infiltration rates of 3, and 5 cm d^{-1} from the AC (7–12 log CFU m L^{-1}) and EC (4–8 log CFU m L^{-1}) columns were less. At these infiltration rates, the leaching cell numbers from the AC and EC columns were significantly lower than FC ($p < 0.001$).

In the FC system, PF2 freely distributed over the columns. The large numbers of the cells were early washed out along with infiltrate at the first PV. Later (2–5 PV), some portion of cells colonized on sand (figure not shown) leading to lower and stable leaching cell numbers. This result well correlated to stable profenofos removal performance by FC (after 4 PV). For AC and EC, higher leaching cells in later period (2–5 PV) may be from the large numbers of cell growing at outer layer of the immobilization materials and being washing off the columns [4]. Even though the high leaching cell numbers were found, the profenofos removal efficiencies did not decrease.

In overall of the short–term results, the profenofos removal by microbial remediation approach was achieved. The free PF2 well degraded profenofos even at the highest infiltration rate (5 cm d^{-1}). This is because PF2 was previously identified as the profenofos-degrading culture [2]. The bacterium is experienced this toxic compound. In practice, the profenofos contamination in environment may be only in several hundreds µg L^{-1}. For example, the profenofos contamination of 950 µg L^{-1} in water from agricultural area in Thailand was reported [14]. At low infiltration rate (1 cm d^{-1}), the free PF2 should be applicable for remediating the profenofos contamination. However, in the case of higher infiltration rates (3–5 cm d^{-1}), profenofos removal efficiencies of FC system were just 50–71%. The use of the FC system might not be able to degrade profenofos to the drinking water quality standard of 0.3 µg L^{-1}.

The immobilized cell systems (AC and EC) could be applied to enhance the profenofos removal. The system is the integrated processes of biodegradation by the immobilized PF2 and adsorption by the materials (peanut shells or barium alginate). During the 5-PV experiment, both AC and EC systems successfully reduced profenofos. Even though it was found the large numbers of PF2 loss in the AC system, there were sufficient numbers of cells colonizing on peanut shells (Fig. 7). Also, peanut shells had suitable surface properties for adsorption [15]. These led to stable profenofos removal.

Even though profenofos removal by BA is statistically lower compared to one by PS ($p < 0.001$), the removal trends presented in Fig. 3 were closed. This well correlated to similar adsorption capabilities (by weight) of PS and BA shown in Table S1. Lower leaching cell number and SEM results in EC system (Figs. 4 and 7) confirmed that the microbial cells were well retained in the entrapment matrices and no apparent restriction of substrate diffusion took place [6]. This could infer that both AC and EC systems have potential for profenofos remediation. The infiltration rates in this study did not significantly influence the profenofos removal performance by the immobilized cell systems for this short-term experiment (5 PV).

Another factor which may influence the profenofos removal is column (cell) depth. A preliminary test of profenofos removal by the free and immobilized cells at different cell depths (10 and 20 cm) was reported in supplementary material (Figs. S3 and S4). It was found that the sand column systems with 10-cm depth (52–80%) could remove profenofos lower than ones with 20-cm depth (50–96%) (Table S3). The change of profenofos removal efficiencies should be because of difference in contact time between contaminant and cell (and the immobilization material). This result revealed that the cell depth may be an important role on the site remediation practice.

3.3. Long-term profenofos removal monitoring

Based on the results of the previous sub-section, it was found that the infiltration rates influenced the profenofos removal by FC. For AC and EC, it was not clear whether adsorption or biodegradation were the main role for profenofos treatment. Therefore, longer period of profenofos

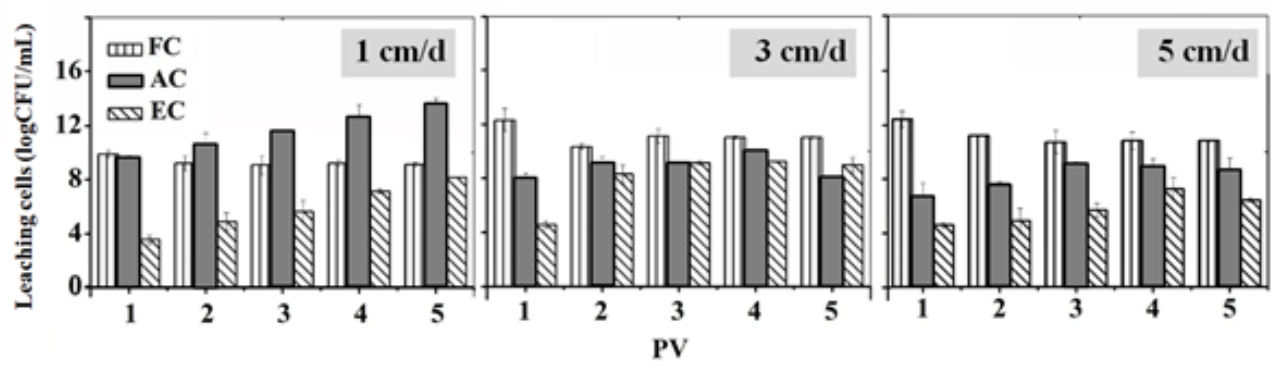

Fig. 4. Leaching cells of the free cell (FC), peanut shell-attached cell (AC), barium alginate-entrapped cell (EC) columns during profenofos removal under infiltration rates of 1, 3, and 5 cm d^{-1}.

removal experiment by sand column at 50 PV (equivalent to 50 d) with the highest infiltration rate of 5 cm d^{-1} was carried out. The columns were continuously fed by simulated contaminated infiltrate with profenofos concentration of 20 mg L^{-1} at hydraulic retention time of 1 d. In the control test (sand only), average profenofos concentration after reaching stable (3–50 PV) was 18.9 mg L^{-1}. This could confirm that natural hydrolysis and degradation did not take place.

The profenofos removal by FC, AC, EC, PS, and BA is presented in Fig. 5. All tests effectively treated profenofos. All columns except BA were reached plateau after 20 PV. The C/C_0 from BA steadily increased during the course of long term experiment. The average profenofos removal efficiencies at a stable period (20–50 PV) are shown in Table 3. Both immobilized cell systems were more effective compared to the free cell system. It was expected to differentiate the role of adsorption and biodegradation on profenofos removal by different immobilized cells (AC and EC). However, it turned out that the performance of both AC and EC systems were comparable.

Fig. 6 presents leaching cell monitoring. For long-term observation, the leaching cells were quite stable for all tests. The AC system (8 log CFU m L^{-1}) had higher leaching cell number compared to one of the EC system (6 log CFU m L^{-1}). The SEM observation (Fig. 7) revealed that a large amount of the microbial cells attached on peanut shells and entrapped inside barium alginate was observed at the beginning. After use for 50 PV, lower amount of cells was observed on AC (Fig. 7b) comparing to EC system (Fig. 7d).

The result from the long-term monitoring warranted achievement of the profenofos removal in this study. After a certain period (5 PV), the profenofos removal by FC increased (Fig. 5). This should be biofilm formation on sand getting to maturation step resulting in higher and constant profenofos removal afterward [16]. For the immobilized cell systems, the profenofos removal was role of biodegradation and adsorption processes. The profenofos removal performance by EC was slightly better than that of AC (Table 3). This is because of high retained cell numbers in EC (less cell wash-out) (Figs. 6 and 7). Additionally, the contaminant

Table 3
Average profenofos removal in the long-term experiment (infiltration rate of 5 cm d^{-1} for 50 days)

Test	Description	Infiltration rate (cm d^{-1})	Profenofos removal (%)
FC	Free cell tests	5	70 ± 3.31
AC	Peanut shell-attached cell tests	5	93 ± 2.21
PS	Peanut shell (no added cell) tests	5	83 ± 1.81
EC	Barium alginate-entrapped cell tests	5	96 ± 0.11
BA	Barium alginate (no added cell) tests	5	80 ± 2.61

1 Numbers after ± referred to standard deviation values.

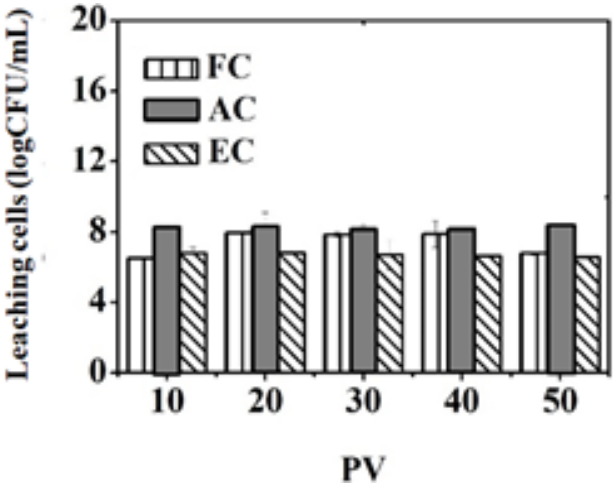

Fig. 6. Leaching cells of the free cell (FC), peanut shell-attached cell (AC), barium alginate-entrapped cell (EC) columns during the long-term profenofos removal experiment at the infiltration rate of 1 cm d^{-1}.

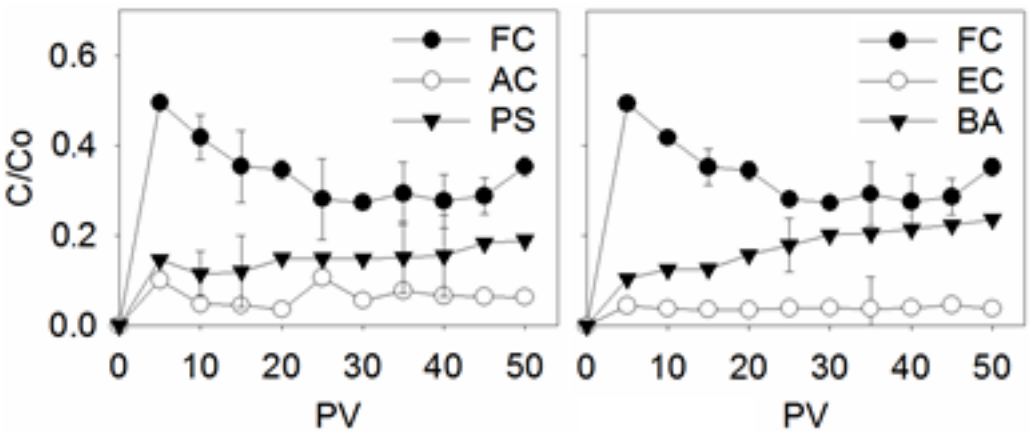

Fig. 5. Breakthrough curves of profenofos removal by the free cell (FC), peanut shell-attached cell (AC), barium alginate-entrapped cell (EC), peanut shell (PS), and barium alginate (BA) tests during the long-term experiment at the infiltration rate of 5 cm d^{-1}.

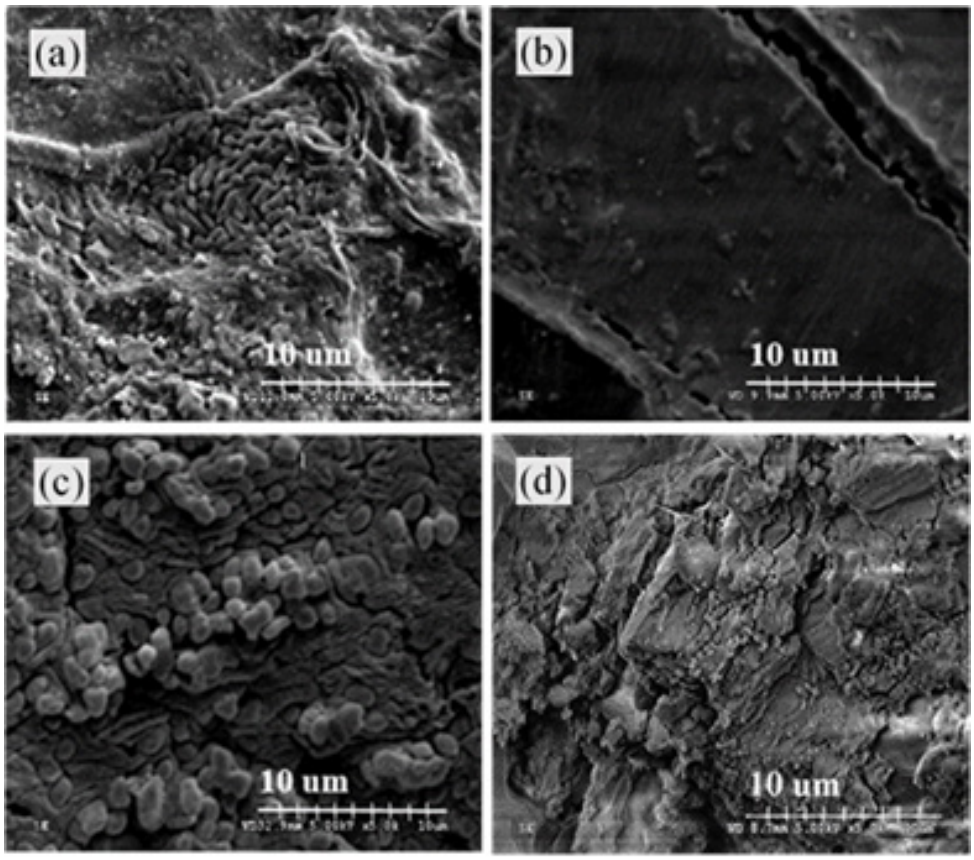

Fig. 7. SEM Observation of the attached cells before (a) and after use for 50 PV (b) and the entrapped cells before (c) and after use for 50 PV (d).

in this study is a toxic substance. Therefore, direct contact at high concentration (20 mg L^{-1}) in FC and AC may damage the microbial cells. The entrapment matrices not only increase cell retention but also reduced impact of substrate toxicity to the cells [17].

Previously, it was indicated that typical primary profenofos degradation product is 4-bromo-2-chlorophenol (BCP). It was known that BCP was higher toxic compared to the parent compound. Siripattanakul-Ratpukdi et al. reported simultaneous profenofos and BCP removal by mixed cultures containing PF2 [2]. This showed potential of PF2 for BCP degradation. Complete profenofos degradation pathway or related toxicity test should be further studied.

In overall, the result from this study could further suggest that the cell retention and contaminant removal efficiency depended on the cell immobilization techniques and the infiltration rates. In practice, it would be difficult to control the infiltration rates. The cell addition technique (free, attached, or entrapped cells) should be considered.

4. Conclusions

The infiltration rates clearly influenced hydraulic transport in sand column. Profenofos remediation by a bacterium culture is promising. At low infiltration rate (1 cm d^{-1}), profenofos well removed in all tests (more than 90%). During the study at higher infiltration rates (3–5 cm d^{-1}), the removal by FC was significantly low (50–71%). The immobilized cell (AC and EC) sand columns effectively removed profenofos (more than 93%) for all tested infiltration rates. As expected, the profenofos remediation by immobilized cells was more efficient than that of the free cells.

In short-term test, AC and EC were found to have similar performance. The two techniques had their own advantages. The cells attached on peanut shells (AC system) had higher adsorption capacity. The profenofos removal by AC was the combination by the attached PF2 and adsorption on the peanut shells. For the EC system, the entrapment matrices had higher cell retention and could lessen profenofos toxicity leading to high biodegradation. For the long-term monitoring, profenofos removal by EC was better than that of AC. In the future, the on-site pilot testing should be investigated for the long-term application under different environmental situations, such as different soil characteristics and weather conditions. The profenofos removal performance and the immobilized cell durability should be further studied.

Acknowledgments

This work was conducted under a research program in Hazardous Substance Management in Agricultural Industry granted by Center of Excellence on Hazardous Substance Management, Thailand. The authors would like to

thank Center for Environmental and Hazardous Substance Management (Khon Kaen University, Thailand), Farm Engineering and Automation Technology Research Group (Khon Kaen University, Thailand), and Khon Kaen University research grant 2016–2017 for financial supports. Any opinions, findings and conclusions or recommendations expressed in this material are those of the author and do not necessarily reflect the views of grant providers.

References

[1] C. Ploychankul, A.S. Vangnai, K. Wantala, S. Siripattanakul-Ratpukdi, Characterization of profenofos degradation by *Pseudomonas plecoglossicida* strain PF1 using surface response methodology, Desal. Water Treat., 89 (2017) 142–149.

[2] S. Siripattanakul-Ratpukdi, A.S. Vangnai, P. Sangthean, S. Singkibut, Profenofos insecticide degradation by novel microbial consortium and isolates enriched from contaminated chili farm soil, Environ. Sci. Pollut. Res., 22 (2015) 320–328.

[3] M. Shakerkhatibi, M. Mosaferi, M.A. Jafarabadi, E. Lotfi, M. Belvasi, Pesticides residue in drinking groundwater resources of rural areas in the northwest of Iran, Health Promot. Perspect., 4 (2014) 195–205.

[4] S. Siripattanakul, W. Wirojanagud, J.M. McEvoy, F.X.M. Casey, E. Khan, Atrazine removal in agricultural infiltrate by bioaugmented polyvinyl alcohol immobilized and free *Agrobacterium radiobacter* J14a: a sand column study, Chemosphere, 74 (2009) 308–313.

[5] Y. Cohen, Bio-filtration of the treatment of fluids by microorganisms immobilized into the filter bedding material: a review, Bioresour. Technol., 77 (2001) 257–274.

[6] S. Siripattanakul, E. Khan, In: Emerging Environmental Technologies Volume 2, Springer, 2010, pp. 147–169.

[7] M. Hazaimeh, S.A. Mutalib, P.S. Abdullah, W.K. Kee, S. Surif, Enhanced crude oil hydrocarbon degradation by self-immobilized bacterial consortium culture on sawdust and oil palm empty fruit bunch, Ann. Microbiol., 64 (2014) 1769–1777.

[8] F. Deng, C. Liao, C. Yang, C. Guo, Z. Dang, Enhanced biodegradation of pyrene by immobilized bacteria on modified biomass materials, Int. Biodeterior. Biodegradation, 110 (2016) 46–52.

[9] A.K. Mathew, M. Crook, K. Chaney, A.C. Humphries, Comparison of entrapment and biofilm mode of immobilisation for bioethanol production from oilseed rape straw using *Saccharomyces cerevisiae* cells, Biomass Bioenergy, 52 (2013) 1–7.

[10] N.C. Olson, J.S. Gulliver, J.L. Nieber, M. Kayhanian, Remediation to improve infiltration into compact soils, J. Environ. Manage., 117 (2013) 85–95.

[11] P. Taweetanawanit, T. Radpukdee, N.T. Giao, S. Siripattanakul-Ratpukdi, Mechanical and chemical stabilities of barium alginate gel: influence of chemical concentrations, Key Eng. Mater., 718 (2017) 62–66.

[12] Z. Bayat, M. Hassanshahian, S. Cappello, Immobilization of microbes for bioremediation of crude oil polluted environments: a mini review, Open Microbiol. J., 9 (2015) 48–54.

[13] P. Sidoli, L. Lassabatere, R. Angulo–Jaramillo, N. Baran, Experimental and modeling of the unsaturated transports of *S*-metolachlor and its metabolites in glaciofluvial vadose zone solids, J. Contam. Hydrol., 190 (2016) 1–14.

[14] K. Harnpicharnchai, N. Chaiear, L. Charerntanyarak, Residues of organophosphate pesticides used in vegetable cultivation in ambient air, surface water and soil in Bueng Niam subdistrict, Khon Kaen, Thailand, Southeast Asian J. Trop. Med. Public Health, 44 (2013) 1088–1097.

[15] Y. Xuan, F.M. Lu, Bioremediation of crude oil-contaminated soil: comparison of different biostimulation and bioaugmentation treatments, J. Hazard. Mater., 183 (2010) 395–401.

[16] M. Berlanga, R. Guerrero, Living together in biofilms: the microbial cell factory and its biotechnological implications, Microb. Cell Fact., 15 (2016) 165.

[17] N.T. Giao, T. Limpiyakorn, P. Kunapongkiti, P. Thuptimdang, S. Siripattanakul-Ratpukdi, Influence of silver nano particles and liberated silver ions on nitrifying sludge: ammonia oxidation inhibitory kinetics and mechanism, Environ. Sci. Pollut. Res., 24 (2017) 9229–9240.

Supporting information

Cell growth and biofilm formation on peanut shells

To prepare the peanut shell-attached cells, the PF2 cells were cultivated in the bacterial medium containing the peanut shells before use. To control equivalent initial cell number for the free, attached, and entrapped cell experiments, the additional test of PF2 growth and biofilm formation on the peanut shells was carried out. The attached cells samples were taken once a day for measuring cell number and biofilm formation potential.

Analytical procedures

Five pieces of the peanut shells with the PF2 cells were washed using a NaCl solution of 0.85%, twice. The washed attached cells were extracted by ultra-sonication and vortex mixing for 2 min each (twice). For cell number count, supernatant was taken for total plate count.

For biofilm formation potential, alcian blue adsorption assay modified from Vandevivere and Kirchman (1993) was performed. Briefly, an alcian blue solution of 1% was added into the washed peanut shells. The mixture was shaken using an orbital shaker at 80 rpm for 15 min. The mixture was filtered using a GF/C filter. The supernatant was measured alcian blue absorbance using spectrophotometer at 606 nm. It is noted that the more alcian blue reduction indicated the more biofilm formation.

Result

Fig. S1 is the results of on PF2 growth and biofilm formation during the preparation of the attached cells used in this study. The PF2 cell number and alcian blue reduction results were well correlated. PF2 increased from approximately 8 to 11 log CFU g-peanut shell^{-1} at the fifth day while biofilm formation (alcian blue reduction) also increased and reached steady state at the same time.

Reference

[1] P. Vandevivere, D.L. Kirchman, Attachment stimulates exopolysaccharide synthesis by a bacterium, Appl. Environ. Microbiol., 59 (1993) 3280–3286.

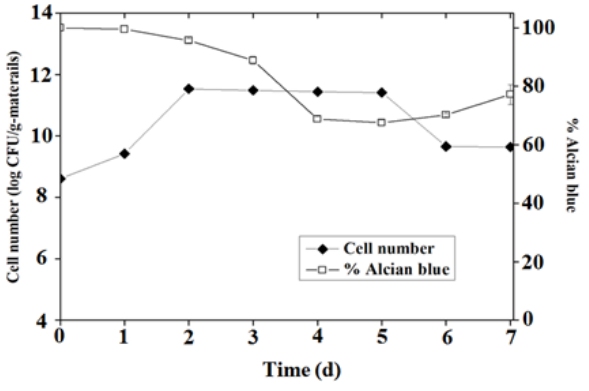

Fig. S1. PF2 cell number and biofilms formation on peanut shells.

Adsorption capability of peanut shells and barium alginate

Adsorption capabilities of PS and BA were preliminarily studied for better interpretation of profenofos removal mechanism. Triplicate batch tests with initial profenofos concentration of 20 mg L^{-1} were performed in an orbital shaker at 150 rpm for 7 d. Fig. S2 clearly proved high profenofos adsorption by PS and BA. Both materials had similar adsorption capability of 1.7–1.8 mg-profenofos g-material^{-1} (Table S2).

It was found that PS and BA of 10 g gave similar profenofos adsorption capability (based on weight) of 1.7 and 1.8 mg-profenofos g-material^{-1}, respectively (Table S2). However, to prepare the materials of 10 g (dried weight), bulk volumes of PS and BA were 10 and 100 mL, respectively (Table S2). This clearly indicated that surface area of these two materials were different. The profenofos removal based on volume of PS and BA were 1.7 and 0.2 mg-profenofos mL^{-1} (Table S2). This could imply that PS had suitable surface properties while BA gave larger surface area. For long-term monitoring (50 PV), PS with better surface properties for profenofos adsorption could maintain profenofos removal performance (Fig. 5).

Comparison of profenofos removal in column at different bed depths

Comparison of column bed depth was preliminarily studied for clearer understanding of profenofos removal mechanism. Triplicate column tests with cell depths of 10 and 20 cm were performed (Fig. S3). It is noted that all columns (10- and 20-cm cell depths) contained the same cell number (and immobilization materials). Fig. S4 is breakthrough curves of profenofos removal by the systems. Table S3 is profenofos removal efficiencies by FC, AC, EC, PS, and BA tests at 5 PV at infiltration rate of 5 cm d^{-1} and different cell depths.

From Fig. S4 results, it is clear that all sand column systems with 10-cm depth could remove profenofos (52–80%). The columns with 10 and 20 cell depths contained the same cell number and amount of immobilization materials; therefore, it gave similar profenofos removal efficiencies.

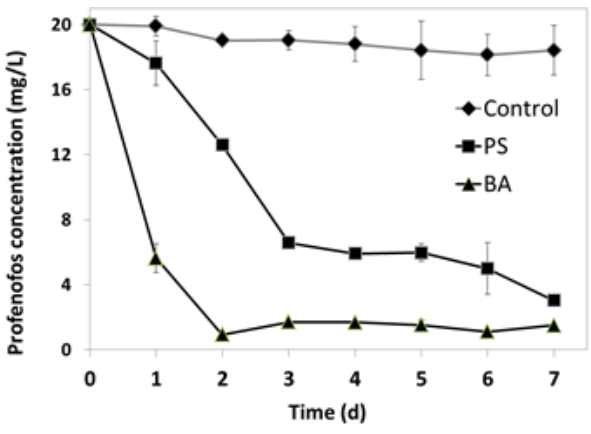

Fig. S2. Profenofos remaining during batch tests.

Table S1
Profenofos removal and adsorption capabilities by PS and BA

Test	Profenofos removal (mg)	Material used (g)	Bulk volume of material (mL)	Profenofos adsorption capability (mg-profenofos/g-material)	Profenofos removal based on volume of PS and BA (mg-profenofos/mL-material)
PS	17	10	10	1.7	1.7
BA	18	10	100	1.8	0.2

Table S2
Profenofos removal efficiencies by FC, AC, EC, PS, and BA tests at 5 PV at infiltration rate of 5 cm d^{-1} and different cell depths

Test	Description	Profenofos removal (%) at cell depth of	
		10 cm	20 cm
FC	Free cell tests	52	50
AC	Peanut shell-attached cell tests	80	90
PS	Peanut shell (no added cell) tests	79	85
EC	Barium alginate-entrapped cell tests	81	96
BA	Barium alginate (no added cell) tests	78	89

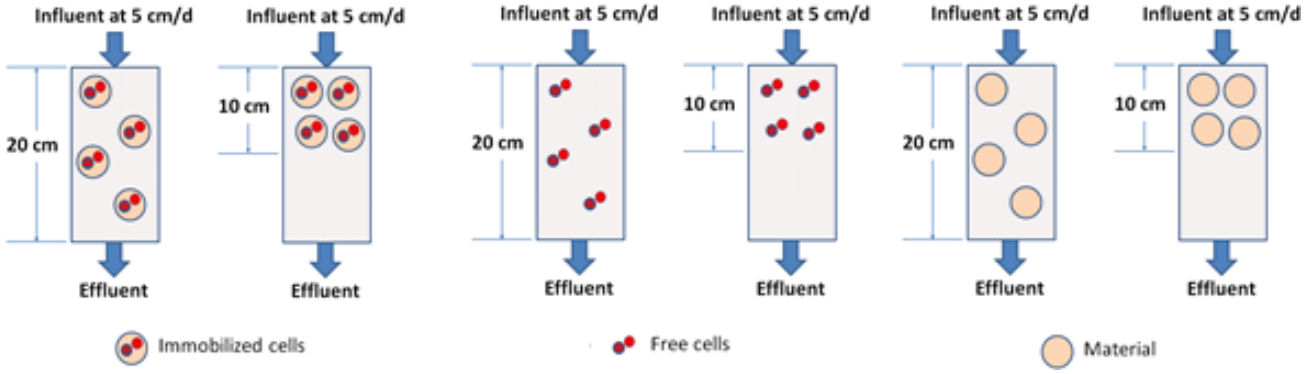

Fig. S3. Schematic diagram of sand column at different cell depths.

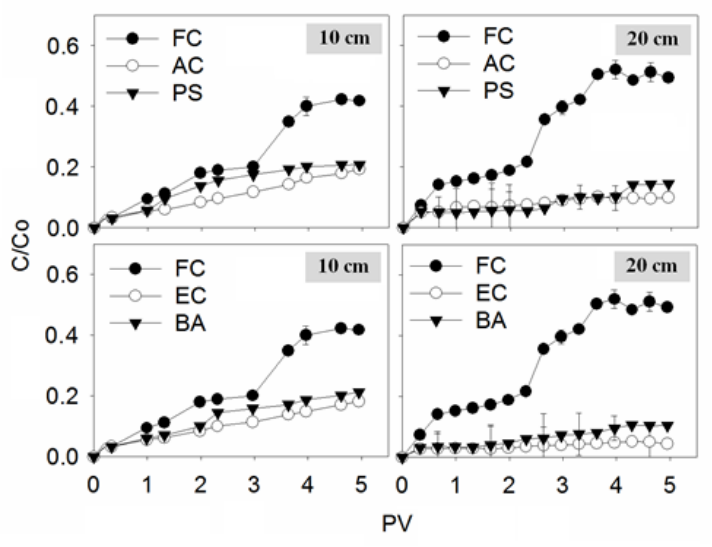

Fig. S4. Breakthrough curves of profenofos removal by the free cell (FC), peanut shell-attached cell (AC), barium alginate-entrapped cell (EC), peanut shell (PS), and barium alginate (BA) tests during the 5-PV experiment at the infiltration rate of 5 cm d^{-1}.

The difference of profenofos removal efficiencies should be because longer column resulted in longer contaminant and cell (and the immobilization material) contact time. The longer contact time should lead to the higher cell growth, contaminant degradation, and contaminant adsorption.

Based on the profenofos removal efficiencies in Table S3, the free cell systems (FC) at different depths did not show the obvious profenofos removal efficiencies. However, profenofos removal by the immobilized cell and only material systems (AC, PS, EC, and BA) apparently increased along with the increasing of the column depth. This may imply that role of bed depth (contact time) sounded important for the immobilized cell systems.